

## Oxygen-Doped Si Epitaxial Films for Si Hetero-Bipolar Transistors

M.Tabe, M.Takahashi and Y.Sakakibara

NTT Electrical Communications Laboratories

3-1, Morinosato Wakamiya, Atsugi, Kanagawa 243-01, Japan

Oxygen-doped Si epitaxial films (OXSEF) on Si (111) substrates have been studied as a new wide gap material for Si hetero-bipolar transistors. It was found that single-crystalline OXSEF with more than 10 at.% oxygen can be grown at 500-700°C under  $O_2$  ambient by means of the Si MBE technique. A  $n^+$ -OXSEF/p-Si diode has been fabricated and its I-V characteristics investigated.

### 1.Introduction

In Si high-speed bipolar transistors, a wide gap emitter instead of the conventional Si emitter is needed to significantly improve the gain. Up to now several kinds of materials have been investigated for hetero-bipolar transistors (HBT).<sup>1-4</sup> None of them, however, seems to be ready for practical use because of difficulties in satisfying a number of requirements. In general, the wide gap material should have a low series resistance and a low density of gap states particularly at the hetero interface. In addition, the material should be able to be formed at low temperatures without affecting underlying impurity profiles.

In this paper, single-crystalline oxygen-doped Si epitaxial films, hereinafter referred to as OXSEF, grown using the Si MBE technique have been studied as a new wide gap material. The typical oxygen concentration in the OXSEF exceeds 10 at.% which probably causes band gap widening, as suggested in previous work on poly or amorphous  $SiO_x$ .<sup>5-7</sup>

### 2.Growth of OXSEF

The apparatus used for OXSEF growth was the Si MBE machine available for 100 mm-wafers previously reported.<sup>8</sup> The OXSEF were grown on Si(111) wafers by means of evaporated Si under  $O_2$  ambient after surface cleaning of the substrate in UHV. The only difference from the conventional Si MBE growth is the presence of  $O_2$  during Si deposition.

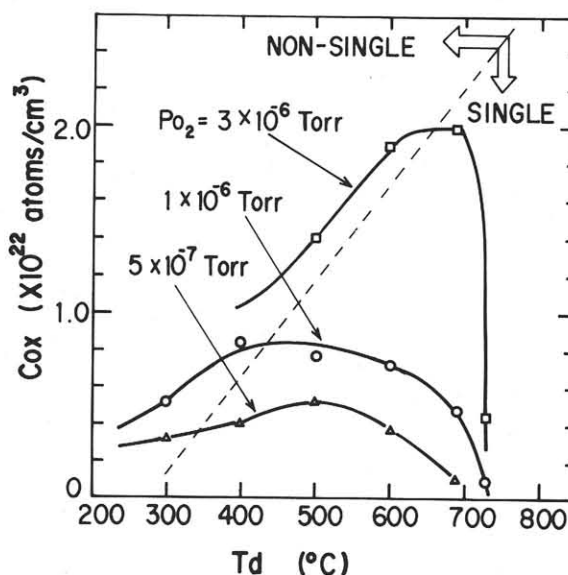


Fig. 1 Oxygen concentration as a function of deposition temperature. The boundary between single and non-single crystalline structures, determined with RHEED, is plotted as the dashed line.

The oxygen concentration ( $C_{ox}$ ) in the grown films determined from IR spectra is plotted in Fig.1 as a function of deposition temperature ( $T_d$ ) for several  $O_2$  pressures ( $P_{O_2}$ ). The film thickness was about 1000 Å. It is natural that the higher  $P_{O_2}$  resulted in the larger  $C_{ox}$ . At a certain  $P_{O_2}$ ,  $C_{ox}$  gradually increases and, after reaching a maximum, rapidly decreases with increasing  $T_d$ . Since the OXSEF growth process can be regarded as repetition of two micro-steps, i.e. deposition of very thin pure Si layer and successive oxidation of its surface,  $C_{ox}(T)$  must be closely related to

the temperature dependence of oxygen adsorption on the clean Si surface. In fact, according to an oxygen adsorption study of the Si(111)7x7 surface,<sup>9)</sup> a similar increase-maximum-decrease dependence of the amount of surface oxygen on temperature was found. The first increase and the later decrease were interpreted as enhancement of oxygen diffusion below the top Si layer and oxygen evaporation in the form of SiO, respectively.

The structure of the films was examined with reflection high-energy-electron diffraction (RHEED). The films were found to be single-crystalline, poly-crystalline or amorphous, depending on growth conditions. The boundary between the single and non-single (poly or amorphous) phases is drawn as the dashed line. In the single region, the RHEED pattern was identical to the Si substrate except for additional {111} twin spots. Therefore we can conclude that these films basically possessed the same structure as the single-crystalline Si and were epitaxially grown with respect to the substrate. To the authors' knowledge, there is only one paper regarding OXSEF growth. Maloney reported that single-crystalline SiO<sub>0.3</sub> was obtained in a very narrow temperature range of 5°C around 675°C under Po<sub>2</sub>=3-5x10<sup>-6</sup> Torr.<sup>10)</sup> His result can be consistently explained by the top curve in Fig.1. That is, C<sub>ox</sub> in the single region rapidly decreases with increasing T<sub>d</sub> under such a high O<sub>2</sub> pressure, confirming the very narrow temperature range for OXSEF growth. One can see from Fig.1 that lower O<sub>2</sub> pressures are desirable in terms of reproducibility of C<sub>ox</sub> because C<sub>ox</sub> is less dependent on T<sub>d</sub>.

The RHEED patterns of the 1000 Å-thick films corresponding to the middle curve in Fig.1 are shown in Fig.2. When the deposition temperature was as low as 300°C ((a)), the halo pattern was observed. In the medium temperature range((b)-(d)), {111} twins were seen as well as the normal spots. At T<sub>d</sub>=690°C((e)) and above, only the normal spots of Si were observed, reflecting the small value of C<sub>ox</sub>. It was also found that the RHEED pattern was dependent not only on T<sub>d</sub> but on film thickness, i.e. the crystallinity was better for thinner layers than thicker layers. In thick layers, however, the crystallinity improved toward the interface, which dominates the device capability. We believe that this point is a prominent difference in comparison with the oxygen-doped poly-crystalline Si, so-called SIPOS.<sup>1)</sup>

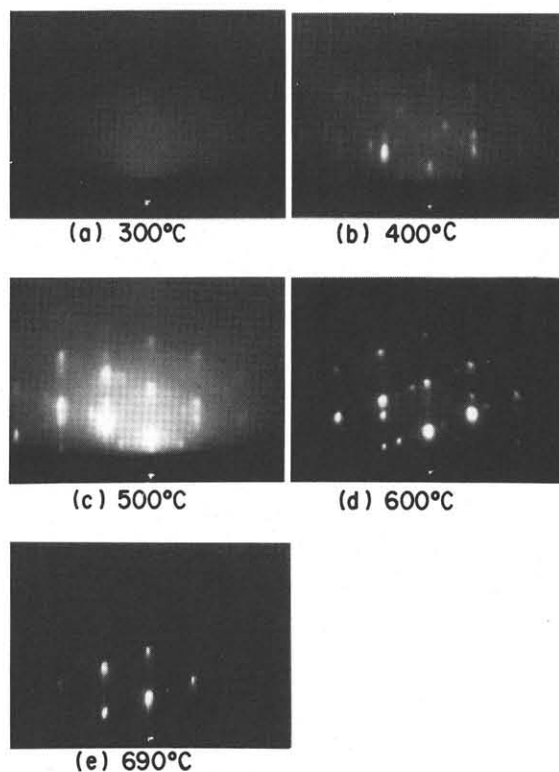


Fig. 2 RHEED patterns of the 1000 Å thick films corresponding to the middle curve in Fig. 1. The incident beam is along the <110> direction.

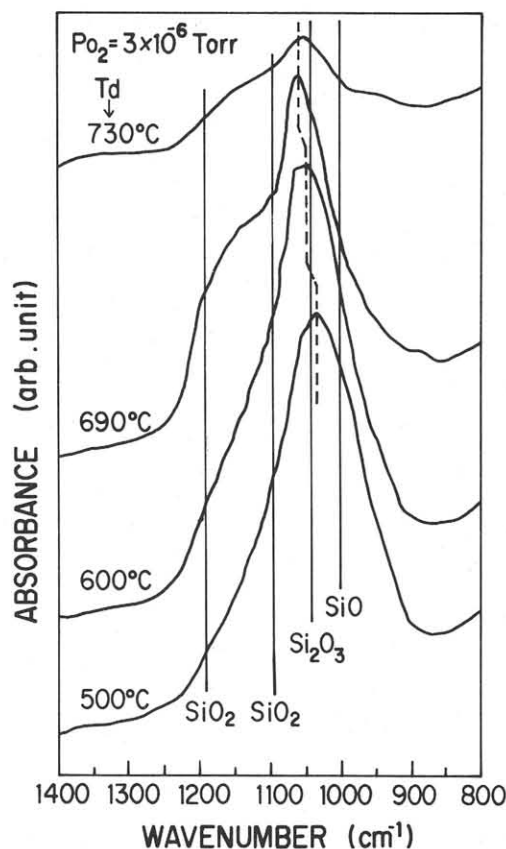


Fig. 3 IR spectra of the samples grown under Po<sub>2</sub>=3x10<sup>-6</sup> Torr.

### 3. Bonding configuration of oxygen

Next we have studied whether the film is phase-separated as a Si-SiO<sub>2</sub> mixture or oxygen is uniformly distributed in the film. In order to answer this question, we have made IR and XPS measurements for different T<sub>d</sub> samples grown under Po<sub>2</sub>=3×10<sup>-6</sup> Torr. Figure 3 shows IR spectra (absorbance) of the samples. The four wave numbers assigned as stretching being due to SiO (1000 cm<sup>-1</sup>),<sup>11)</sup> Si<sub>2</sub>O<sub>3</sub> (1040 cm<sup>-1</sup>),<sup>11)</sup> and thermally grown SiO<sub>2</sub> (1096, 1190 cm<sup>-1</sup>)<sup>12)</sup> are also shown. It is seen that the peak wave number changed with increasing T<sub>d</sub> from 1030 to 1060 cm<sup>-1</sup>, indicating that the major compound was nearly Si<sub>2</sub>O<sub>3</sub> but slightly moved toward SiO<sub>2</sub>. It should be noted, however, that the peak position is still lower than that of SiO<sub>2</sub> even for the highest T<sub>d</sub>. Unfortunately, there is some ambiguity in the above assignment, because porosity and strain in the film possibly shift the peak position.<sup>11)</sup>

Therefore, we made an XPS measurement of Si-2p core level to confirm the determination of oxygen configuration by the IR measurement. The results are shown in Fig. 4. In order to avoid the influence of native oxide, 200 Å of the surface was sputtered with Ar prior to the measurement. The shaded area is the contribution from chemically shifted Si-2p bonded to one to four oxygen atoms as indicated by the arrows. It is evident that in all samples incomplete oxides were dominant rather than SiO<sub>2</sub> and that the contribution from more complete oxide slightly increased with increasing T<sub>d</sub> being consistent with

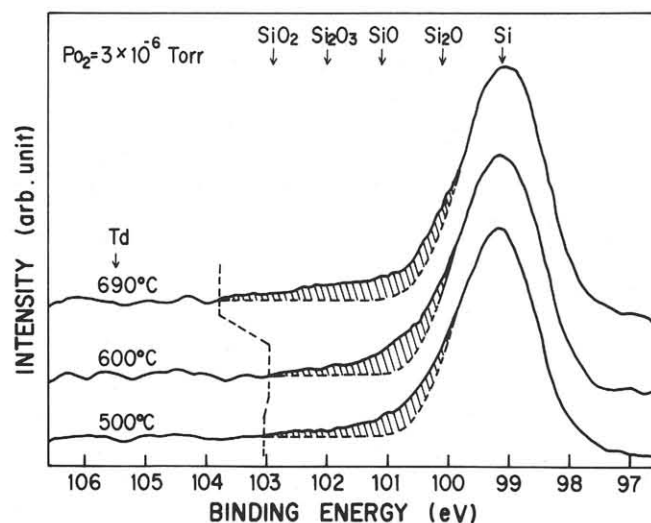


Fig. 4 Si-2p core level spectra for the same samples as in Fig. 3. The shaded area is due to shifted peaks.

Fig. 3. It is difficult to explain the reason why the major contribution seemed to arise from SiO in XPS instead of Si<sub>2</sub>O<sub>3</sub> in IR. Because the effect of Ar sputtering on the composition and the chemical shift is not well known. From these figures, however, we can derive the following qualitative conclusion: oxygen atoms are incorporated as an incomplete oxide, like Si<sub>2</sub>O<sub>3</sub> or SiO, and the films are not fully phase-separated as Si+SiO<sub>2</sub>. In addition, the oxide slightly moved toward SiO<sub>2</sub> with increasing deposition temperature, but it is still far from SiO<sub>2</sub>.

### 4. Oxygen depth profile and its annealing effect

The oxygen profile in the OXSEF grown at T<sub>d</sub>=500°C under Po<sub>2</sub>=1×10<sup>-6</sup> Torr is plotted in Fig. 5 (a) using Auger electron spectroscopy. Oxygen profiles after 30 min-annealing in N<sub>2</sub> at 800 and 1000°C are also plotted. These profiles imply that a large amount of oxygen has penetrated into the film from the surface but the deep step-like profile is preserved. This penetration probably took place during the loading and unloading time for the thermal treatment. Therefore, the OXSEF might include voids somewhat as previously reported for UHV-deposited amorphous Si. It is obvious, however, that a single-crystalline Si cap of 200 Å on top of the OXSEF is very effective in avoiding the oxygen penetration, as shown in Fig. 5 (b). The Si cap was successively deposited at the same temperature after the OXSEF growth.

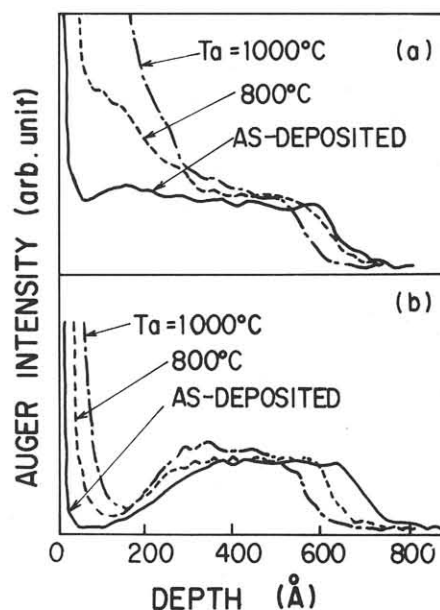


Fig. 5 Oxygen depth profiles before and after N<sub>2</sub> annealing (a) without and (b) with a 200 Å single-crystalline Si cap.

## 5. Diode characteristics

In order to examine the device capability of the OXSEF, we have fabricated a  $n^+$ -OXSEF/p-Si diode with a structure shown in Fig.6. The fabrication steps are briefly summarized below.

- (i) 0.1  $\mu$ -thick OXSEF was deposited on a boron-doped ( $1 \times 10^{18} \text{ cm}^{-3}$ ) Si substrate at  $T_d = 500^\circ\text{C}$  under  $P_{O_2} = 1 \times 10^{-6}$  Torr.
- (ii) After the LOCOS process ( $900^\circ\text{C}$  130 min), 0.3  $\mu$ -thick undoped poly Si was deposited.
- (iii) Arsenic as an n-type impurity was introduced into the poly Si by ion implantation (100 keV,  $5 \times 10^{16} \text{ cm}^{-2}$ ).
- (iv) Then, the sample was annealed in two steps ( $850^\circ\text{C}$  10 min and  $900^\circ\text{C}$  120 min) to allow As to diffuse into the OXSEF.
- (v) finally, Al was deposited on top and patterned.

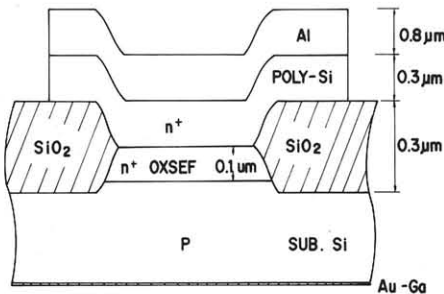


Fig. 6 Schematic structure of  $n^+$ -OXSEF/p-Si diode.

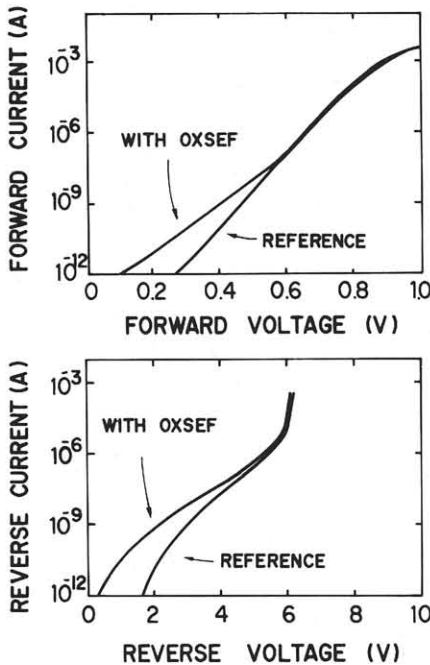


Fig. 7 Forward and reverse I-V characteristics of the OXSEF and the reference diodes.

Although it is difficult to precisely locate the p-n junction with respect to the hetero interface, the p-n junction was found by SIMS to be several hundreds angstroms beyond the hetero interface. As a reference, a diode without OXSEF was also fabricated. The process was the same as the OXSEF diode except that poly Si was directly deposited on the substrate.

The I-V curves for these two diodes are shown in Fig.7, where the upper figure is the forward and the lower figure is the reverse characteristic with a different voltage scale. Although generation-recombination current contribution is appreciable for the OXSEF diode in the low voltage region, a good rectification was obtained.  $N_A$  values evaluated from the forward current at around 0.7 V were 1.13 for the OXSEF and 1.03 for the reference. The breakdown voltage in both curves is about 6 V which is due to avalanche breakdown dominated by the substrate impurity concentration. Further analyses such as temperature dependence of the I-V curves are now being done and the result will be published soon.

## Acknowledgment

The authors would like to thank to T.Sakai for valuable discussions and encouragement. Also, they are grateful to N.Owada and M.Kondo for their continuous support.

## References

- 1) T.Matsushita, N.Ohuchi, H.Hayashi and H.Yamoto, Appl.Phys.Lett., 35, 549 (1979).
- 2) M.Ghannam, J.Nijs, R.Mertens and R.Dekeersmaecker, IEDM Tech.Dig., p.746 (1984).
- 3) K.Sasaki, S.Furukawa and M.M.Rahman, IEDM Tech.Dig., p.294 (1985).
- 4) T.Sugii, T.Ito, M.Doki, F.Mieno, Y.Furumura and M.Maeda, VLSI Technol., Dig. of Tech. Papers
- 5) M.Hamazaki, T.Adachi, S.Wakayama and M.Kikuchi, Solid State Communications, 21, 591 (1977).
- 6) H.R.Philipp, J.Phys.Chem.Solids, 32, 1935 (1971).
- 7) A.J.Bennett and L.M.Roth, Phys.Rev., B4, 2686 (1971).
- 8) M.Tabe, J.Vac.Sci.Technol., B3, 975 (1985).
- 9) M.Tabe, T.Chiang, I.Lindau and W.E.Spicer, Phys.Rev., to be published.
- 10) T.J.Maloney, J.Vac.Sci.Technol., B1, 773 (1983).
- 11) W.A.Pliskin, Thin Solid Films, 2, 1 (1968).
- 12) N.Nagasima, Jpn.J.Appl.Phys., 9, 879 (1970).